

General Relativistic Description of the Observed Galaxy Power Spectrum: Do We Understand What We Measure?

Jaiyul Yoo*

Harvard-Smithsonian Center for Astrophysics, Harvard University, 60 Garden Street, Cambridge, MA 02138

We extend the general relativistic description of galaxy clustering developed in Yoo, Fitzpatrick, and Zaldarriaga (2009). For the first time we provide a fully general relativistic description of the observed matter power spectrum and the observed galaxy power spectrum with the linear bias ansatz. It is significantly different from the standard Newtonian description on large scales and especially its measurements on large scales can be misinterpreted as the detection of the primordial non-Gaussianity even in the absence thereof. The key difference in the observed galaxy power spectrum arises from the real-space matter fluctuation defined as the matter fluctuation at the hypersurface of the observed redshift. As opposed to the standard description, the shape of the observed galaxy power spectrum evolves in redshift, providing additional cosmological information. While the systematic errors in the standard Newtonian description are negligible in the current galaxy surveys at low redshift, correct general relativistic description is essential for understanding the galaxy power spectrum measurements on large scales in future surveys with redshift depth $z \geq 3$. We discuss ways to improve the detection significance in the current galaxy surveys and comment on applications of our general relativistic formalism in future surveys.

PACS numbers: 98.80.-k, 98.65.-r, 98.80.Jk, 98.62.Py

I. INTRODUCTION

Measurements of the galaxy power spectrum can be used to infer the shape of the primordial matter power spectrum, providing valuable clues to understand the initial conditions of early universe. In the linear regime, galaxy bias — the relation between the galaxy and the underlying matter distributions — is fairly generic and simple that the shape of the observed galaxy power spectrum reflects the shape of the matter power spectrum [1]. Therefore, recent theoretical work [2–5] has focused on interpreting the galaxy power spectrum measurements from quasilinear scales to nonlinear scales where the measurement precision is highest, yet galaxy bias is significantly affected by the complex nature of galaxy formation physics.

However, the past decades have seen a rapid growth in this field, and large-scale galaxy surveys such as the Sloan Digital Sky Survey (SDSS; [6]) now cover a substantial fraction of the entire sky over a range of redshift, allowing for measurements of the galaxy power spectrum on sufficiently large scales with unprecedented precision [7–9]. Recently, Dalal et al. [10] showed that the shape of the galaxy power spectrum in the linear regime contains a very distinctive feature in the presence of the primordial non-Gaussianity. These very large-scale modes of the galaxy power spectrum are already measured with high signal-to-noise ratios from the SDSS, putting tight constraints on the amplitude of the primordial non-Gaussianity [11], comparable to the limits from the Wilkinson Microwave Anisotropy Probe (WMAP). Further theoretical work [11–17] shows that future galaxy surveys can measure the galaxy power spectrum on large scales with the accuracy enough to detect the small non-Gaussianity from the simplest single field inflationary models [18] and the

nonlinear evolution of the Gaussian spectrum [19].

The contribution of the primordial non-Gaussianity to the galaxy power spectrum mainly arises from the gravitational potential and this relativistic contribution becomes comparable to the contribution of the matter fluctuation on large scales. However, at this large scale, where the relativistic effects become dominant, the standard Newtonian description of the galaxy power spectrum breaks down and the general relativistic description is therefore essential for understanding the observed galaxy power spectrum and deriving correct constraints from the measurements. Furthermore, there exists subtlety in theoretical calculations in this regime, where general relativistic effects are important: Since the general covariance provides a large number of degrees of freedom, many theoretical descriptions of observable quantities turn out to have unphysical gauge freedoms and they fail to correctly describe observable quantities that we measure on large scales. Naturally, these systematic errors in those theoretical calculations are negligible in the Newtonian limit, but they become substantial on large scales [20].

Fully general relativistic descriptions should be constructed by using observable quantities, rather than theoretically convenient but unobservable quantities as they are gauge-dependent. The gauge-invariance is a necessary condition for observable quantities and it should be used for the consistency check of theoretical calculations of observable quantities. For example, the observable quantities in the galaxy clustering case are the observed redshift, the observed galaxy position on the sky, and the total number of observed galaxies. Yoo, Fitzpatrick, and Zaldarriaga [20] developed a general relativistic description of galaxy clustering and applied it to the cross-correlation of large-scale structure with CMB temperature anisotropies, in which the largest scale modes can be most effectively probed. On low angular multipoles, the correct relativistic prediction of the cross-correlation is larger by about a factor two than the standard Newtonian prediction, alleviating the discrepancy between the theoretical prediction and the

*jyoo@cfa.harvard.edu

anomalously large signal measured from the SDSS and the WMAP data (e.g., see [21]).

Here we compute the observed galaxy power spectrum, accounting for all the general relativistic effects but we only focus on the linear regime, where the general relativistic effect is substantial. The observed galaxy power spectrum shows significant difference on large scales, compared to the standard description, i.e., the biased matter power spectrum in the synchronous gauge with the redshift-space distortion effect [22]. The correct “real-space” matter power spectrum is anisotropic and the shape of the observed galaxy power spectrum changes with redshift. Especially, its measurements on large scales can result in a false detection of the primordial non-Gaussianity even in the absence thereof.

The organization of this paper is as follows. In Sec. II we compute the real-space matter power spectrum accounting for the relativistic effects and we discuss its stark difference from the matter power spectrum in the synchronous gauge. We extend the calculation of the real-space matter power spectrum to computing the full observed galaxy power spectrum in Sec. III A and we forecast the detectability of the departure of the observed galaxy power spectrum from the standard prediction in the current and future galaxy surveys in Sec. III B. We summarize our new findings and discuss the implication of our results for the proposed future surveys in Sec. IV.

The detailed and technical calculations of our results are presented in two Appendices. In Appendix A we summarize our notation convention and discuss the gauge issues associated with metric representations. Calculations of observable quantities are presented in Appendix B with particular emphasis on the gauge-invariance of each equation. In computing our results, we assume there is no vector or tensor mode, while we present general formulas with vector and tensor modes. We use the Boltzmann code CMBFast [23] to obtain the transfer functions of perturbation variables.

II. REAL-SPACE MATTER POWER SPECTRUM

The general relativistic description of the observed galaxy number density n_g is derived in [20] and we rearrange the expression in terms of gauge-invariant variables defined in Appendix A as

$$n_g = \bar{n}_p(z) \left[1 + b m_{\delta z} + \alpha_\chi + 2 \varphi_\chi + V - C_{\alpha\beta} e^\alpha e^\beta \right. \\ \left. + 3 \delta z_\chi + 2 \frac{\delta \mathcal{R}}{r_s} - H \frac{\partial}{\partial z} \left(\frac{\delta z_\chi}{\mathcal{H}} \right) - 5p \delta \mathcal{D}_L - 2 \mathcal{K} \right], \quad (1)$$

where \bar{n}_p is the mean galaxy number density in a homogeneous universe and each term in the square bracket represents contributions from the volume distortion and the source effect (see Appendix B).

In this section we compute the contribution of the matter fluctuation $m_{\delta z} = \delta_m - 3 \delta z$ to the observed galaxy power spectrum. While the matter fluctuation itself is not directly observable, computing the matter power spectrum $P_{m_{\delta z}}(\mathbf{k})$ merits close investigation, since $m_{\delta z}$ is boosted by a galaxy

bias factor b separating it from the rest of the contributions in Eq. (1) and its simple but gauge-invariant structure provides a guideline for computing the full observed galaxy power spectrum using Eq. (1). More importantly, $P_{m_{\delta z}}(\mathbf{k})$ is the dominant contribution to the observed galaxy power spectrum on all scales.

Therefore, we consider the matter fluctuation at the hypersurface defined by the observed redshift z

$$m_{\text{dm}} n_{\text{dm}}(z, \hat{\mathbf{n}}) = \bar{\rho}_m(t)(1 + \delta_m) = \bar{\rho}_m(z)(1 + m_{\delta z}), \quad (2)$$

where $\hat{\mathbf{n}}$ is the observed position on the sky, δz is the lapse in the observed redshift (see Appendix B) and we assume $m_{\text{dm}} \equiv 1$ hereafter. Of particular importance is the distinction between δ_m and $m_{\delta z}$. The former δ_m , commonly referred to as the matter fluctuation, is a *gauge-dependent* quantity and its meaning is ambiguous because the time slicing is unspecified. For example, the same matter density ρ_m can result in different values of δ_m due to the change in the mean matter density $\bar{\rho}_m(t)$ in different coordinate systems (note that $\bar{\rho}_m(t)$ is just a function of coordinate time t). However, the latter $m_{\delta z}$, also we call the matter fluctuation (at the observed redshift), is gauge-invariant and unambiguously defined, since the time slicing is set by the observed redshift z , rather than by an arbitrary choice of coordinate systems as for δ_m . This perspective provides a theoretical ground for what ought to be the correct quantity for the so-called “real-space” matter power spectrum $P_{m_{\delta z}}(\mathbf{k})$.¹

In computing the matter power spectrum, we need to compute the observed mean $\langle n_{\text{dm}} \rangle_\Omega$ and the observed matter fluctuation $\hat{m}_{\delta z} \equiv n_{\text{dm}} / \langle n_{\text{dm}} \rangle_\Omega - 1$.² The need to distinguish $\hat{m}_{\delta z}$ from $m_{\delta z}$ arises from the ambiguity of quantities at origin in $m_{\delta z}$. The full expression of $m_{\delta z}$ is (see Appendix B)

$$m_{\delta z} = (\delta_m + 3 H \chi) - 3 (\mathcal{H} \delta \tau + H \chi)_o - 3 \left[V - \alpha_\chi \right]_o^s \\ + 3 \int_0^{r_s} dr \left[(\alpha_\chi - \varphi_\chi)' - (\Psi_{\alpha|\beta} + C'_{\alpha\beta}) e^\alpha e^\beta \right], \quad (3)$$

¹ There are two widely known gauge-invariant variables for the matter fluctuation ϵ_m and ϵ_g defined in Bardeen [24], where $\epsilon_m = \delta_m + 3(1+w)\mathcal{H}(v+k\beta)/k$ and $\epsilon_g = \delta_m + 3(1+w)\mathcal{H}(\beta+\gamma')$ (see Appendix A for our notation convention). They describe the matter fluctuation in the matter rest frame ($v+k\beta=0$) and in the zero shear frame ($\chi=0$), respectively (ϵ_m and ϵ_g correspond to δ_v and δ_χ in our notation). However, in practice there is no theoretical reason to prefer one gauge condition to other conditions. The time slicing in observation is set by the (gauge-invariant) observed redshift z , and hence the matter fluctuation $m_{\delta z}$ in this frame correctly represents the “observed” matter fluctuation (note that $m_{\delta z} = \delta_m$ in the uniform-redshift gauge $\delta z=0$). Furthermore, all the above gauge-invariant variables ϵ_m , ϵ_g , and $m_{\delta z}$ are different on large scales (see Fig. 1), and the gauge-invariance is not a sufficient condition for observable quantities.

² For an observed number density field $n(z, \hat{\mathbf{n}})$ at the observed redshift z , the observed mean $\langle n \rangle_\Omega$ is obtained by averaging n over all angle $\hat{\mathbf{n}}$ within the survey area Ω , i.e., averaging over the hypersurface of simultaneity set by the observed redshift z . However, the usual ensemble average, also commonly denoted as $\langle n \rangle$, is obtained by averaging n over the hypersurface set by the coordinate time t , and hence it is gauge-dependent. The observed mean and the theoretical mean (ensemble average) should be carefully distinguished.

and it contains quantities evaluated at origin such as the time lapse $\delta\tau_o$ and so on. However, as noted in Yoo, Fitzpatrick, and Zaldarriaga [20], these quantities are nuisance in observation due to their independence of the observed angle $\hat{\mathbf{n}}$: They are absorbed to the observed mean $\langle n_{\text{dm}} \rangle_\Omega$ and subtracted from n_{dm} to give $\hat{m}_{\delta z}$ without the ambiguities at origin (note that in observation $\hat{m}_{\delta z}$ is derived from the observed number density n_{dm}).

Though implicit in most theoretical calculations, we explicitly account for this observational procedure. The observed mean number density is therefore

$$\begin{aligned} \langle n_{\text{dm}} \rangle_\Omega &= \int_\Omega d^2\hat{\mathbf{n}} n_{\text{dm}}(z, \hat{\mathbf{n}}) / \int_\Omega d^2\hat{\mathbf{n}} \\ &\simeq \bar{\rho}_m(z) \left[1 - 3(\mathcal{H}_o \delta\tau_o + H_o \chi_o) + 3(V - \alpha_\chi)_o \right], \end{aligned} \quad (4)$$

where $V = V_\alpha e^\alpha$. In the last equality, we assumed that perturbation variables that vary with the observed angle $\hat{\mathbf{n}}$ would vanish when averaged over angle within the survey area Ω . However, this assumption is valid only if the survey area is infinite: Modes of wavelength larger than the survey scale would not average out but set a constant floor in the observed mean. Collectively, Eq. (4) may have additional constant. However, since this additional constant is also independent of observed position $\hat{\mathbf{n}}$ and gauge-invariant, it has no impact on the power spectrum computation, and we can safely assume that there is no further contribution in Eq. (4). Also, note the subtle difference $\langle n_{\text{dm}} \rangle_\Omega \neq \bar{\rho}_m(z) \neq \langle n_{\text{dm}} \rangle = \bar{\rho}_m(t)$, but their difference is at the level of metric perturbations.

Therefore, the observed matter fluctuation can be written as

$$\begin{aligned} \hat{m}_{\delta z} &\equiv n_{\text{dm}} / \langle n_{\text{dm}} \rangle_\Omega - 1 = (\delta_m + 3H\chi) + 3(\alpha_\chi - V) \\ &+ 3 \int_0^{r_s} dr \left[(\alpha_\chi - \varphi_\chi)' - (\Psi_{\alpha|\beta} + C'_{\alpha\beta}) e^\alpha e^\beta \right]. \end{aligned} \quad (5)$$

Now we can make a gauge choice and compute the matter power spectrum $P_{\hat{m}_{\delta z}}(\mathbf{k})$.³ By inspecting Eq. (5), it proves most convenient to compute the matter power spectrum in the conformal Newtonian gauge ($\chi = 0$),

$$\hat{m}_{\delta z} = \delta_m^N + 3\psi - 3V + 3 \int_0^{r_s} dr \left[(\psi - \phi)' - H_{\alpha\beta}^{T'} e^\alpha e^\beta \right], \quad (6)$$

where $\alpha_\chi = \alpha (\equiv \psi)$, $\varphi_\chi = \varphi (\equiv \phi)$ in the conformal Newtonian gauge. We emphasize that $\hat{m}_{\delta z}$ computed by using Eq. (6) is gauge-invariant, i.e., its value is identical to those computed by using Eq. (5) with any other choice of gauge conditions. Finally, the matter power spectrum can be computed

³ Choosing a gauge condition per se has nothing unphysical nor incorrect. In fact, it is desirable for numerical convenience. The key point is that one has to be careful in relating theoretical predictions to observable quantities, for which the gauge-invariance is a necessary condition. However, by choosing a gauge condition before deriving equations, one loses an explicit way to check the gauge-invariance of theoretical predictions, and the predictions become gauge-dependent when they involve unobservable quantities.

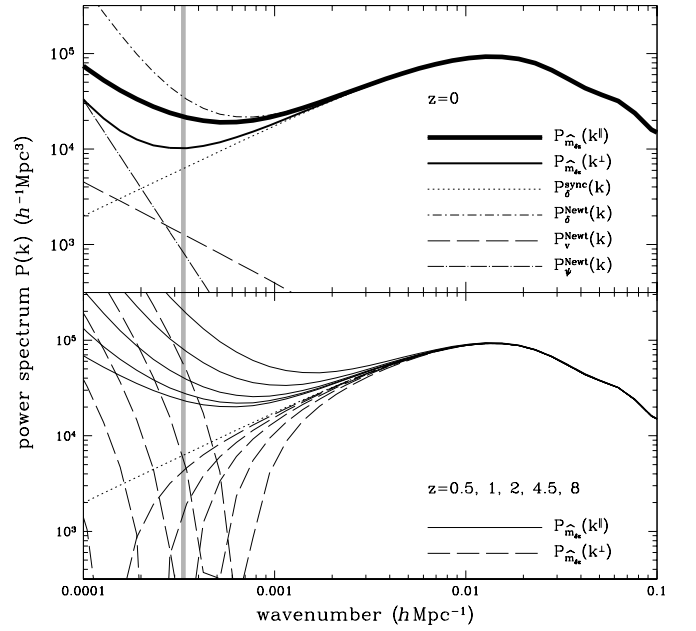


FIG. 1: Matter power spectrum $P_{\hat{m}_{\delta z}}(k, \mu_k)$ at various redshifts. Upper panel: Solid lines represent the matter power spectrum at $z = 0$, computed by using Eq. (7) along the line-of-sight direction ($\mu_k = 1$; thick) and along the transverse direction ($\mu_k = 0$; thin). For reference, various lines indicated in the legend show power spectra of perturbation variables in the conformal Newtonian gauge and the synchronous gauge. Bottom panel: matter power spectrum $P_{\hat{m}_{\delta z}}(k, \mu_k)$ at $z > 0$, but with its amplitude normalized to match $P_{\hat{m}_{\delta z}}(k, \mu_k)$ at $z = 0$. Solid and dashed lines represent $P_{\hat{m}_{\delta z}}(k, \mu_k)$ with $\mu_k = 1$ and $\mu_k = 0$, respectively. The horizon scale at $z = 0$ is shown as a vertical line.

as

$$\begin{aligned} P_{\hat{m}_{\delta z}}(\mathbf{k}) &= P_\phi(k) T_{\hat{m}_{\delta z}}(\mathbf{k}, z) T_{\hat{m}_{\delta z}}^*(\mathbf{k}, z) \\ &\simeq P_m^N(k) + 9 P_\psi(k) + 6 P_{m\psi}(k) + 9 \mu_k^2 P_v(k), \end{aligned} \quad (7)$$

where $P_\phi(k)$ is the power spectrum of the primordial curvature perturbations and $T_{\hat{m}_{\delta z}}$ is the transfer function for $\hat{m}_{\delta z}$ (we will use T_X to refer to the transfer function for the perturbation variable X). We ignored the complication due to survey geometry, and the redshift dependence of each power spectrum term in the second line is suppressed for notational simplicity. Since projected quantities such as the integrated Sachs-Wolfe effect in Eq. (6) are intrinsically angular quantities, they are nearly independent of the line-of-sight mode k^{\parallel} due to the Limber cancellation of the small scale modes, and we have ignored these contributions in computing Eq. (7).

Solid lines in the upper panel of Fig. 1 represent the matter power spectrum $P_{\hat{m}_{\delta z}}(k, \mu_k)$ along the line-of-sight and the transverse directions. With the time slicing set by the observed redshift z , the “real-space” matter power spectrum $P_{\hat{m}_{\delta z}}(\mathbf{k})$ is no longer isotropic, and it is neither the matter power spectrum $P_\delta^S(k)$ in the synchronous gauge (dotted), nor $P_\delta^N(k)$ in the conformal Newtonian gauge (dot-dashed). Since the synchronous gauge corresponds to the dark matter rest frame, $P_\delta^S(k)$ would be what we measure if we knew their

positions without measuring redshift z . However, the (coordinate) positions in the synchronous gauge are also gauge-dependent quantities, and we need the observed redshift z to define the time slicing and their observed positions. On small scales $k \gg 10\mathcal{H}$, the matter power spectrum $P_{\hat{m}_{\delta z}}(k, \mu_k)$ becomes virtually isotropic, and the difference in $P_{\delta}(k)$ with various gauge conditions vanishes compared to the correct matter power spectrum $P_{\hat{m}_{\delta z}}(k, \mu_k)$.

The bottom panel shows the matter power spectrum $P_{\hat{m}_{\delta z}}(k, \mu_k)$ at high redshifts $z = 0.5, 1, 2, 4.5, 8$ along the line-of-sight direction (solid) and along the transverse direction (dashed). Compared to $P_{\hat{m}_{\delta z}}(k^{\perp})$ at $z = 0$, significant difference is immediately noticeable along the transverse direction, where the matter power spectrum has the zero-crossing scale at each redshift. Along the transverse direction, the matter fluctuation is $\hat{m}_{\delta z} \simeq \delta_m^N + 3\psi$. Since the matter fluctuation δ_m^N decreases with redshift but the gravitational potential $\psi (< 0)$ remains nearly constant, the matter fluctuation $\hat{m}_{\delta z}$ becomes zero and changes its sign on large scales, and this zero-crossing scale becomes smaller at higher redshift. Physically, the magnitude of the lapse δz in the observed redshift is larger than the density fluctuation δ_m on large scales, such that the change in the mean matter density $\bar{\rho}_m(t)$ overwhelms the density fluctuation and hence $\hat{m}_{\delta z}$ appears to be underdense in observation. The matter power spectrum $P_{\hat{m}_{\delta z}}(k^{\parallel})$ along the line-of-sight direction maintains the similar trend at $z = 0$ shown in the upper panel. However, compared to the matter power spectrum $P_{\delta}^S(k)$ in the synchronous gauge (dotted), the turn-off scale of $P_{\hat{m}_{\delta z}}(k, \mu_k)$ becomes smaller, as the horizon size decreases with redshift.

III. OBSERVED GALAXY POWER SPECTRUM

A. Theoretical Prediction

Having computed the real-space matter power spectrum in Sec. II, we are now in a position to tackle the full complexity of the observed galaxy number density n_g in Eq. (1). Following the same procedure, we compute the observed mean galaxy number density by considering contributions independent of the observed galaxy position,

$$\langle n_g \rangle_{\Omega} = \bar{n}_p \left[1 + b m_{\delta z_o} + 3 \delta z_{\chi_o} + 2 \frac{\delta \mathcal{R}_o}{r_s} - 5p \delta \mathcal{D}_{L_o} - 2 \mathcal{K}_o \right], \quad (8)$$

where the surface terms in each component are

$$\delta z_{\chi_o} = (\mathcal{H}_o \delta \tau_o + H_o \chi_o) - (V - \alpha_{\chi})_o, \quad (9)$$

$$m_{\delta z_o} = -3 \delta z_{\chi_o},$$

$$\delta \mathcal{R}_o = (\chi_o + \delta \tau_o) - \frac{\delta z_{\chi_o}}{\mathcal{H}},$$

$$\delta \mathcal{D}_{L_o} = (\mathcal{H}_o \delta \tau_o + H_o \chi_o) + \left(\frac{\chi_o + \delta \tau_o}{r_s} \right) - \frac{\delta z_{\chi_o}}{\mathcal{H} r_s},$$

$$\mathcal{K}_o = e_{\alpha} (\delta e_{\chi}^{\alpha} + \Psi^{\alpha} + 2 C_{\beta}^{\alpha} e^{\beta})_o.$$

Therefore, the observed galaxy fluctuation can be obtained by subtracting the observed mean as

$$\begin{aligned} \delta_g &= n_g / \langle n_g \rangle_{\Omega} - 1 = b (m_{\delta z} - m_{\delta z_o}) + \alpha_{\chi} + 2 \varphi_{\chi} \quad (10) \\ &+ V - C_{\alpha\beta} e^{\alpha} e^{\beta} + 3 (\delta z_{\chi} - \delta z_{\chi_o}) + 2 \left(\frac{\delta \mathcal{R} - \delta \mathcal{R}_o}{r_s} \right) \\ &- H \frac{\partial}{\partial z} \left(\frac{\delta z_{\chi}}{\mathcal{H}} \right) - 5p (\delta \mathcal{D}_L - \delta \mathcal{D}_{L_o}) - 2 (\mathcal{K} - \mathcal{K}_o). \end{aligned}$$

This equation maintains the gauge-invariant structure, yet lacks any ambiguity at origin.

As discussed in Sec. II, we make simplifications to facilitate computing the observed galaxy power spectrum $P_g(k, \mu_k)$ by adopting a simple survey geometry, ignoring contributions from the projected quantities, and choosing the conformal Newtonian gauge ($\chi = 0$). The observed galaxy power spectrum is therefore

$$P_g(\mathbf{k}) = P_{\phi}(k) T_g(\mathbf{k}, z) T_g^*(\mathbf{k}, z), \quad (11)$$

with the transfer function

$$\begin{aligned} T_g &= b (T_m^N + 3 T_{\psi} - 3 T_V) + T_{\psi} + 2 T_{\phi} + T_V \\ &+ 3 (T_V - T_{\psi}) + 2 \left(\frac{T_{\psi} - T_V}{\mathcal{H} r_s} \right) - H \frac{\partial}{\partial z} \left(\frac{T_V - T_{\psi}}{\mathcal{H}} \right) \\ &- 5p \left(T_V - T_{\psi} + \frac{T_{\psi} - T_V}{\mathcal{H} r_s} \right) \\ &= b T_m^N + \mathcal{N} T_{\psi} - \frac{T_{\phi'}}{\mathcal{H}} - \mu_k^2 \frac{k T_v}{\mathcal{H}} + i \mu_k \mathcal{M} T_v, \quad (12) \end{aligned}$$

where two coefficients in the transfer function are

$$\begin{aligned} \mathcal{N} &= 3b - 1 + \frac{1+z}{H} \frac{dH}{dz} + (5p - 2) - \left(\frac{5p - 2}{\mathcal{H} r_s} \right), \\ \mathcal{M} &= 3b + \frac{1+z}{H} \frac{dH}{dz} + (5p - 2) - \left(\frac{5p - 2}{\mathcal{H} r_s} \right). \quad (13) \end{aligned}$$

Finally, the observed galaxy power spectrum in Eq. (11) is

$$\begin{aligned} P_g(k, \mu_k) &= b^2 P_m^N(k) + \mathcal{N}^2 P_{\psi}(k) + 2 b \mathcal{N} P_{m\psi}(k) \\ &+ \mu_k^2 \left[\mathcal{M}^2 P_v(k) - \frac{2 b k}{\mathcal{H}} P_{mv}(k) - \frac{2 \mathcal{N} k}{\mathcal{H}} P_{\psi v}(k) \right] \\ &+ \mu_k^4 \frac{k^2}{\mathcal{H}^2} P_v(k), \quad (14) \end{aligned}$$

where we ignored the contribution from $T_{\phi'}/\mathcal{H}$, which vanishes quickly at $z > 0$. With our fiducial cosmology these coefficients range $\mathcal{N} - 3b = -0.5 \sim 0.5$ and $\mathcal{M} - 3b = 0.8 \sim 1.5$ for the luminosity function slope $5p = 2$ of the source galaxy sample, where the source effect is minimized.⁴ The observed galaxy power spectrum $P_g(k, \mu_k)$ is therefore approximately the biased matter power spectrum $b^2 P_{\hat{m}_{\delta z}}(k, \mu_k)$ with

⁴ The source effect cannot be exactly cancelled on all scales, even for the case $5p = 2$, because the fluctuation $\delta \mathcal{D}_L$ in the luminosity distance reduces to the standard convergence κ only in the Newtonian limit, i.e., $5p \delta \mathcal{D}_L + 2 \mathcal{K} \neq 0$ on large scales, even when $5p = 2$.

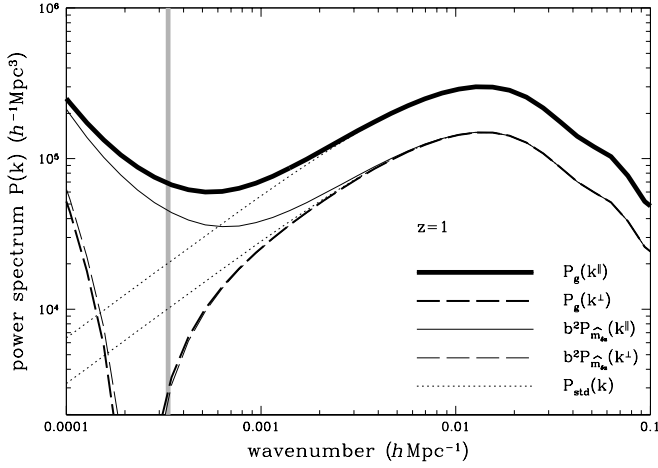


FIG. 2: Observed galaxy power spectrum $P_g(k, \mu_k)$ at $z = 1$. Thick lines represent the observed galaxy power spectrum, computed by using the full general relativistic description in Eq. (14) along the line-of-sight direction ($\mu_k = 1$; solid) and along the transverse direction ($\mu_k = 0$; dashed). Dotted lines show the observed galaxy power spectrum using the standard method in Eq. (15). For comparison, the matter power spectrum $b^2 P_{\hat{m}_{\delta z}}(k, \mu_k)$ is shown as thin lines with the galaxy bias factor $b = 2$.

the standard redshift-space distortion factor, in which case two coefficients are exactly $\mathcal{N} = 3b$, $\mathcal{M} = 3b$ (when $5p = 2$ is assumed).

In comparison, the observed galaxy power spectrum and its transfer function in the standard method are

$$\begin{aligned} P_{\text{std}}(k, \mu_k) &= P_\phi(k) T_{\text{std}}(\mathbf{k}, z) T_{\text{std}}^*(\mathbf{k}, z) \\ &= b^2 P_\delta^S(k) - \mu_k^2 \frac{2bk}{\mathcal{H}} P_{\delta v}(k) + \mu_k^4 \frac{k^2}{\mathcal{H}^2} P_v(k), \end{aligned} \quad (15)$$

and

$$T_{\text{std}} = b T_m^S - \mu_k^2 \frac{k T_v}{\mathcal{H}}, \quad (16)$$

respectively. The standard transfer function T_{std} is composed of two transfer functions (T_m^S and T_v) in two different gauge conditions, one in the synchronous gauge and one in the conformal Newtonian gauge.

Figure 2 shows the observed galaxy power spectrum $P_g(k, \mu_k)$ at $z = 1$, computed by using Eq. (14). As we noted in Sec. II, the matter power spectrum $P_{\hat{m}_{\delta z}}(k, \mu_k)$ is the dominant contribution to the observed galaxy power spectrum on all scales, and the redshift-space distortion from the volume distortion enhances the power. Along the transverse direction (thick dashed), the observed galaxy power spectrum $P_g(k^\perp)$ largely traces the biased real-space matter power spectrum $b^2 P_{\hat{m}_{\delta z}}(k^\perp)$ (thin dashed) as the standard description of the observed galaxy power spectrum (lower dotted) is the biased matter power spectrum in the synchronous gauge $P_{\text{std}}(k^\perp) = b^2 P_\delta^S(k)$. However, on large scales, the standard description overestimates the observed galaxy power spectrum along the transverse direction due to the contribution of δz in $P_{\hat{m}_{\delta z}}(k^\perp)$. Similarly, the observed

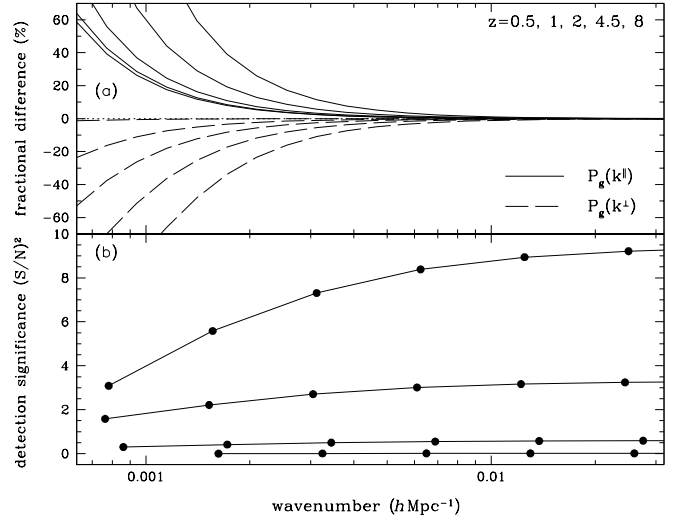


FIG. 3: Systematic errors in theoretical modeling of the observed galaxy power spectrum. Upper panel: fractional difference of $P_g(k, \mu_k)$ at various redshift slices, compared to the standard description $P_{\text{std}}(k, \mu_k)$ in Eq. (15) along the line-of-sight direction (solid) and along the transverse direction (dashed). Bottom panel: detection significance of the departure from the standard description in a cosmic-variance limited survey as a function of maximum wavenumber. The survey volume is divided into four spherical shells with redshift range $z = 0 \sim 1$ (bottom solid), $1 \sim 3$, $3 \sim 6$, and $6 \sim 10$ (top solid), and the signal is computed at the mean redshift of each shell.

galaxy power spectrum $P_g(k^\parallel)$ along the line-of-sight direction (thick solid) significantly deviates from the standard description $P_{\text{std}}(k^\parallel) = (b + f)^2 P_\delta^S(k)$ (upper dotted) on large scales, where f is the growth rate of structure. The deviation arises mainly from the difference between $b^2 P_{\hat{m}_{\delta z}}(k^\parallel)$ and $b^2 P_\delta^S(k)$, but there exists small contribution from the volume distortion in addition to the standard redshift-space distortion effect.

Figure 3a compares the correct galaxy power spectrum $P_g(k, \mu_k)$ in Eq. (14) with respect to the standard description $P_{\text{std}}(k, \mu_k)$ in Eq. (15) at various redshift slices. Solid and dashed lines represent the fractional difference $\Delta P_g / P_{\text{std}} = P_g / P_{\text{std}} - 1$ along the line-of-sight direction ($\mu_k = 1$; solid) and along the transverse direction ($\mu_k = 0$; dashed), respectively. On large scales $k \leq 0.01 h \text{Mpc}^{-1}$, the standard description underestimates the observed galaxy power spectrum along the line-of-sight direction and overestimates along the transverse direction. At higher redshift, the fractional difference in the observed galaxy power spectrum at a fixed wavenumber is progressively amplified, because the relativistic effects increase as the horizon size becomes smaller. A few percent deviation is already present at $k = 0.01 h \text{Mpc}^{-1}$ at $z \geq 4.5$.

B. Statistical uncertainties on power spectrum measurements

Of the utmost importance is the detectability of the systematic errors in theoretical modeling of the observed galaxy power spectrum $P_g(k, \mu_k)$ on large scales. We consider statistical uncertainties on measurements of the two-dimensional anisotropic power spectrum by using a simple mode counting approximation. Since Fourier modes are effectively independent of each other, the statistical uncertainty decreases with $1/\sqrt{N_k}$, where N_k is the number of Fourier modes available given a survey volume V_s . However, sampling of individual galaxies contributes the shot noise errors $1/\langle n_g \rangle_\Omega$ to the signal $P_g(k, \mu_k)$, and the number of independent Fourier modes is in fact a half of N_k as $\delta_g(\mathbf{k})$ represents a real quantity in configuration space. Therefore, the statistical uncertainty of each Fourier mode is [25, 26]

$$\left(\frac{\sigma_p}{P_g}\right)^2 = \frac{2}{V_k V_{\text{eff}}}, \quad (17)$$

and the detection significance of the departure in the observed galaxy power spectrum from the standard method prediction is

$$\left(\frac{S}{N}\right)^2 = \left(\frac{\Delta P_g}{\sigma_p}\right)^2 = \left(\frac{\Delta P_g}{P_{\text{std}}}\right)^2 \left(\frac{V_k V_{\text{eff}}}{2}\right), \quad (18)$$

where $\Delta P_g = P_g - P_{\text{std}}$,

$$V_k = \frac{2\pi \Delta(k^\perp)^2 \Delta k^\parallel}{(2\pi)^3}, \quad (19)$$

is the Fourier volume accounting for the positive and negative k^\parallel , and the effective survey volume is

$$V_{\text{eff}} = \int dV_s \left[\frac{\langle n_g \rangle_\Omega P_g}{1 + \langle n_g \rangle_\Omega P_g} \right]^2. \quad (20)$$

For definiteness we consider galaxy samples measured from a large-scale survey with full sky coverage (cosmic-variance limited) as a function of survey redshift depth. We choose the galaxy number density $\langle n_g \rangle_\Omega = 10^{-4} (h^{-1} \text{Mpc})^{-3}$, similar to what the current large-scale surveys aim to measure (e.g., [27]). Since the shot noise contribution is small $\langle n_g \rangle_\Omega P_g \geq 1$ on scales of our interest $k \leq 0.01 h \text{Mpc}^{-1}$, the effective volume in Eq. (20) is therefore identical to the survey volume $V_{\text{eff}} \simeq V_s$. Here we assume a flat Λ CDM universe with the matter density $\Omega_m = 0.24$, the baryon density $\Omega_b = 0.042$, the Hubble constant $h = 0.73$, the spectral index $n_s = 0.954$, the optical depth to the last scattering surface $s = 0.09$, and the primordial curvature perturbation amplitude $\Delta_\phi^2 = 2.38 \times 10^{-9}$ at $k = 0.05 \text{Mpc}^{-1}$ ($\sigma_8 = 0.81$).

The significance $(S/N)^2$ of the systematic errors as a function of maximum wavenumber is shown in Fig. 3b, where we divide the survey volume into four spherical shells, covering the full sky with redshift range $z = 0 \sim 1$, $1 \sim 3$, $3 \sim 6$, and $6 \sim 10$. At the lowest redshift bin ($z = 0 \sim 1$), the survey

volume is $V_s = 58 (h^{-1} \text{Gpc})^3$ and the minimum wavenumber is $k_{\text{min}} = \Delta k = 2\pi/V_s^{1/3} = 0.0016 h \text{Mpc}^{-1}$, at which the fractional difference is 8% along the line-of-sight direction (solid) and is close to zero along the transverse direction (dashed) as shown in Fig. 3a. With only a handful of modes at k_{min} , the systematic errors in theoretical modeling of the observed galaxy power spectrum is negligible at $z \leq 1$ (bottom solid line in Fig. 3b). Similar conclusion can be derived for the survey volume at $z = 1 \sim 3$ (second solid line from the bottom).

However, at the higher redshift bins (two upper solid lines), there exist two critical differences in assessing the significance of the systematic errors: Larger survey volume and smaller horizon size. About a factor of ten larger volume is available in the higher redshift bins than in the lowest redshift bin, which reduces the statistical uncertainties at a fixed k by $10^{1/2} \simeq 3.2$ and provides k_{min} smaller by $10^{1/3} \simeq 2.2$. Furthermore, the relativistic effects are larger at a fixed k due to the smaller horizon size at the higher redshift bins, increasing the fractional difference $\Delta P_g/P_{\text{std}}$ at each k . Consequently, the significance of the systematic errors increases dramatically with survey redshift depth.

In conclusion, the volume available at $z \leq 3$ is less than the Hubble volume and hence the standard Newtonian description is statistically indistinguishable from the general relativistic description of the observed galaxy power spectrum at $z \leq 3$. However, the systematic errors in theoretical modeling increase substantially with redshift and correct general relativistic description is essential in understanding the observed galaxy power spectrum at $z \geq 3$.

In practice, further complication will be present for measuring the largest scale modes in galaxy surveys, because they are affected by survey window functions and large contiguous region is required. Long line-of-sight modes are relatively immune to these difficulties, while modeling the redshift evolution of galaxy bias may complicate the theoretical interpretation of the observed galaxy power spectrum $P_g(k^\parallel)$ along the line-of-sight direction. Proper application of our method to observations will require further investigation with close ties to the specifications of a given survey geometry.

IV. DISCUSSION

We have extended the general relativistic description of galaxy clustering developed in Yoo, Fitzpatrick, and Zaldarriaga [20] and we have provided, for the first time, the correct general relativistic description of the observed galaxy power spectrum with particular emphasis on the expressions for observable quantities and their gauge-invariance. In the galaxy clustering case, the observable quantities involve the observed redshift z , the galaxy position $\hat{\mathbf{n}}$ on the sky, the number N_{tot} of observed galaxies, and its apparent luminosity L . These quantities are different from the quantities defined in a homogeneous and isotropic universe, which are theoretically more tractable, yet unobservable (gauge-dependent) quantities. The gauge-invariance is a necessary condition for observable quantities and the observed galaxy power spectrum

should be expressed in terms of the observable quantities.

There are two key contributions to the observed galaxy power spectrum: The real-space matter fluctuation and the volume distortion. While the standard redshift-space distortion effect accounts for most of the contributions from the volume distortion, the former requires a careful definition of its meaning and it exhibits significant difference on large scales compared to the standard real-space matter fluctuation. Since the observed redshift z defines the hypersurface of simultaneity in observation, the correct description of the real-space matter fluctuation is the matter fluctuation at the observed redshift, $m_{\delta z} = \delta_m - 3 \delta z$ ($m_{\delta z} = \delta_m$ in the uniform-redshift frame $\delta z = 0$). As it is defined by observable quantities, $m_{\delta z}$ is naturally gauge-invariant, in contrast to the usual (gauge-dependent) matter fluctuation δ_m , which requires a specification of gauge conditions or coordinate systems and differs in its value contingent upon the gauge choice.

As the observed redshift z depends on angle, the real-space matter power spectrum $P_{m_{\delta z}}(\mathbf{k})$ is no longer isotropic: Compared to the matter power spectrum $P_{\delta}^S(k)$ in the synchronous gauge, $P_{m_{\delta z}}(\mathbf{k})$ is enhanced along the line-of-sight direction but it is suppressed along the transverse direction, because the lapse δz in the observed redshift can increase or decrease the mean matter density, affecting δ_m in both direction. Consequently, the shapes of the real-space matter power spectrum $P_{m_{\delta z}}(\mathbf{k})$ and the observed galaxy power spectrum vary with redshift at $k \leq 0.01h\text{Mpc}^{-1}$, while the shape of the matter power spectrum $P_{\delta}^S(k)$ in the synchronous gauge is independent of redshift. Therefore, a proper modification is necessary for methods to use the multipole moments of the observed galaxy power spectrum on large scales to constrain the growth factor of the matter fluctuation. Traditionally, measurements of the observed galaxy power spectrum at different redshift slices are combined to reduce the statistical uncertainties, but with the redshift evolution of the power spectrum shape on large scales, they can be used to extract additional cosmological information.

Recently, it is shown [10] that the primordial non-Gaussianity in gravitational potential can give rise to the scale-dependence of the observed galaxy power spectrum on large scales, where galaxy bias is assumed to be linear. Furthermore, it is guaranteed [12, 17, 28] that future galaxy surveys will detect non-Gaussian signatures on large scales, arising from either primordial or nonlinear evolution. However, its signature on large scales is similar to the rising power of the real-space matter power spectrum $P_{m_{\delta z}}(\mathbf{k})$ in Fig. 1 and the observed galaxy power spectrum in Fig. 2, since they all originate from the contribution of the gravitational potential. Therefore, without proper theoretical modeling of the observed galaxy power spectrum, its measurements on large scales can be misinterpreted as the detection of the primordial non-Gaussianity even in the absence thereof, and its false detection can be used as the evidence against the simplest single field inflationary models. With the full general relativistic description of the observed galaxy power spectrum developed

here, the effect of the primordial non-Gaussianity on the observed galaxy power spectrum will be investigated in a separate work.

While the current galaxy surveys cover a large fraction of the entire sky, it is still difficult to directly measure the departure of the observed galaxy power spectrum from the standard description at $z \leq 3$ with high significance, simply due to the limited number of large-scale modes. However, recent work [29] suggested a method to eliminate the cosmic variance errors by comparing two different biased tracers. The scale-dependence of the ratio of two galaxy power spectra arises from the volume distortion: Unlike in the standard description of the primordial non-Gaussianity, all biased traces depend on the same matter fluctuation $m_{\delta z}$ and hence there would be no scale-dependence, if it were not for the volume distortion. With substantial increase in the signal-to-noise ratio, current galaxy surveys may be able to detect the general relativistic effects in the observed galaxy power spectrum at low redshift.

In future galaxy surveys with larger redshift depth, correct general relativistic description should be an essential element in power spectrum analysis, as significant systematic errors will be present in the standard description of the observed galaxy power spectrum due to smaller horizon size and larger survey volume at high redshift. Furthermore, our formalism can be easily extended to any alternative theories of gravity. Since these theories are identical in the Newtonian limit but have distinctive relativistic effects, alternative theories of gravity can be most effectively probed on cosmological scales. Comparison of their theoretical predictions to the galaxy power spectrum measurements on large scales can, therefore, provide a way to test general relativity and put constraints on the alternative.

While we considered a spectroscopic galaxy survey here, a majority of planned large-scale surveys such as the Dark Energy Survey (DES), the Panoramic Survey Telescope & Rapid Response System (PanSTARRS), and the Large Synoptic Survey Telescope (LSST) lack of observationally expensive spectroscopic instruments, and instead they rely on photometric redshift measurements. However, the degradation of redshift measurement precision will have little impact on the detectability of large-scale modes, since it only results in radial smearing of galaxy positions ($\Delta r \leq 100h^{-1}\text{Mpc}$ at $z = 1$, and smaller at higher redshift) and the general relativistic effect appears on large scales $k \leq 0.01h\text{Mpc}^{-1}$.

Acknowledgments

J.Y. acknowledges useful discussions with Daniel Eisenstein, Eiichiro Komatsu, Uroš Seljak, and Michael Turner. Especially, J.Y. thanks Matias Zaldarriaga for his encouragement and critical comments throughout the completion of this work. J. Y. is supported by the Harvard College Observatory under the Donald H. Menzel fund.

- [1] N. Kaiser, *Astrophys. J. Lett.* **284**, L9 (1984).
- [2] R. E. Smith, J. A. Peacock, A. Jenkins, S. D. M. White, C. S. Frenk, F. R. Pearce, P. A. Thomas, G. Efstathiou, and H. M. P. Couchman, *Mon. Not. R. Astron. Soc.* **341**, 1311 (2003), arXiv:astro-ph/0207664.
- [3] J. Yoo, D. H. Weinberg, J. L. Tinker, Z. Zheng, and M. S. Warren, *ArXiv e-prints* (2008), 0808.2988.
- [4] P. McDonald, *Phys. Rev. D* **74**, 103512 (2006), arXiv:astro-ph/0609413.
- [5] M. Crocce and R. Scoccimarro, *Phys. Rev. D* **73**, 063519 (2006), arXiv:astro-ph/0509418.
- [6] D. G. York et al., *Astron. J.* **120**, 1579 (2000), arXiv:astro-ph/0006396.
- [7] M. Tegmark et al., *Phys. Rev. D* **74**, 123507 (2006), arXiv:astro-ph/0608632.
- [8] B. A. Reid, W. J. Percival, D. J. Eisenstein, L. Verde, D. N. Spergel, R. A. Skibba, N. A. Bahcall, T. Budavari, M. Fukugita, J. R. Gott, et al., *ArXiv e-prints* (2009), 0907.1659.
- [9] N. P. Ross, T. Shanks, R. D. Cannon, D. A. Wake, R. G. Sharp, S. M. Croom, and J. A. Peacock, *Mon. Not. R. Astron. Soc.* **387**, 1323 (2008), arXiv:0704.3739.
- [10] N. Dalal, O. Doré, D. Huterer, and A. Shirokov, *Phys. Rev. D* **77**, 123514 (2008), 0710.4560.
- [11] A. Slosar, C. Hirata, U. Seljak, S. Ho, and N. Padmanabhan, *J. Cosmol. Astropart. Phys.* **8**, 31 (2008), 0805.3580.
- [12] P. McDonald, *Phys. Rev. D* **78**, 123519 (2008), 0806.1061.
- [13] S. Matarrese and L. Verde, *Astrophys. J. Lett.* **677**, L77 (2008), 0801.4826.
- [14] A. L. Fitzpatrick, L. Senatore, and M. Zaldarriaga, *ArXiv e-prints* (2009), 0902.2814.
- [15] D. Jeong and E. Komatsu, *Astrophys. J.* **703**, 1230 (2009), 0904.0497.
- [16] V. Desjacques and U. Seljak, *Phys. Rev. D* **81**, 023006 (2010), 0907.2257.
- [17] N. Afshordi and A. J. Tolley, *Phys. Rev. D* **78**, 123507 (2008), 0806.1046.
- [18] J. Maldacena, *J. High Energy Phys.* **5**, 13 (2003), arXiv:astro-ph/0210603.
- [19] T. Pyne and S. M. Carroll, *Phys. Rev. D* **53**, 2920 (1996), arXiv:astro-ph/9510041.
- [20] J. Yoo, A. L. Fitzpatrick, and M. Zaldarriaga, *Phys. Rev. D* **80**, 083514 (2009), 0907.0707.
- [21] S. Ho, C. Hirata, N. Padmanabhan, U. Seljak, and N. Bahcall, *Phys. Rev. D* **78**, 043519 (2008), 0801.0642.
- [22] N. Kaiser, *Mon. Not. R. Astron. Soc.* **227**, 1 (1987).
- [23] U. Seljak and M. Zaldarriaga, *Astrophys. J.* **469**, 437 (1996), astro-ph/9603033.
- [24] J. M. Bardeen, *Phys. Rev. D* **22**, 1882 (1980).
- [25] H. A. Feldman, N. Kaiser, and J. A. Peacock, *Astrophys. J.* **426**, 23 (1994), arXiv:astro-ph/9304022.
- [26] M. Tegmark, *Phys. Rev. Lett.* **79**, 3806 (1997), arXiv:astro-ph/9706198.
- [27] D. J. Eisenstein, J. Annis, J. E. Gunn, A. S. Szalay, A. J. Connolly, R. C. Nichol, N. A. Bahcall, M. Bernardi, S. Burles, F. J. Castander, et al., *Astron. J.* **122**, 2267 (2001), arXiv:astro-ph/0108153.
- [28] C. Carbone, L. Verde, and S. Matarrese, *Astrophys. J. Lett.* **684**, L1 (2008), 0806.1950.
- [29] U. Seljak, *Phys. Rev. Lett.* **102**, 021302 (2009), 0807.1770.
- [30] J.-C. Hwang and H. Noh, *Phys. Rev. D* **65**, 023512 (2001), arXiv:astro-ph/0102005.
- [31] J. M. Bardeen, in *Cosmology and Particle Physics*, edited by L. Fang and A. Zee (Gordon and Breach, London, 1988), p. 1.
- [32] M. Sasaki, *Mon. Not. R. Astron. Soc.* **228**, 653 (1987).

Appendix A: FLRW metric and notation convention

We summarize our notation convention for the most general metric in an inhomogeneous Friedmann-Lemaître-Robertson-Walker (FLRW) universe and we discuss the gauge transformation properties and gauge freedoms of the perturbation variables used in this paper.

The background universe is described by a spatially homogeneous and isotropic metric with scale factor $a(t)$,

$$ds^2 = g_{ab} dx^a dx^b = -dt^2 + a^2(t) \bar{g}_{\alpha\beta} dx^\alpha dx^\beta, \quad (\text{A1})$$

where $\bar{g}_{\alpha\beta}$ is the metric tensor for a three-space with a constant spatial curvature $K = -H_0^2 (1 - \Omega_{\text{tot}})$. We extensively use the conformal time τ , defined as $a(\tau) d\tau = dt$. Throughout the paper, we use the Latin indices for the spacetime component and the Greek indices for the spatial component, and we set the speed of light $c \equiv 1$.

Small departure of the metric tensor in the inhomogeneous universe from the background metric can be represented as a set of metric perturbations:

$$\begin{aligned} \delta g_{00} &= -2 a^2 \alpha, \\ \delta g_{0\alpha} &= -a^2 \mathcal{B}_\alpha = -a^2 (\beta_{,\alpha} + B_\alpha), \\ \delta g_{\alpha\beta} &= 2 a^2 \mathcal{C}_{\alpha\beta} = 2 a^2 (\varphi \bar{g}_{\alpha\beta} + \gamma_{\alpha|\beta} + C_{(\alpha|\beta)} + C_{\alpha\beta}), \end{aligned} \quad (\text{A2})$$

where the vertical bar represents the covariant derivative with respect to spatial metric $\bar{g}_{\alpha\beta}$, and the perturbation classification from its transformation properties is represented with single or double indices for vector-type or tensor-type, respectively. We adopt the classification scheme introduced in [24].

The general covariance in general relativity guarantees that any coordinate system can be used to describe physical systems and the choice of a coordinate system bears no physical significance. A coordinate transformation accompanies a change in the correspondence of the real physical (inhomogeneous) universe to the homogeneous background universe, known as the gauge transformation. Here we consider the most general coordinate transformation

$$\tilde{x}^a = x^a + \xi^a, \quad (\text{A3})$$

where $\xi^a = (T, \mathcal{L}^\alpha)$ and $\mathcal{L}^\alpha = L'^\alpha + L^\alpha$. Under the coordinate transformation, the scalar metric perturbations transform as

$$\begin{aligned} \tilde{\alpha} &= \alpha - T' - \mathcal{H} T, \\ \tilde{\beta} &= \beta - T + L', \\ \tilde{\varphi} &= \varphi - \mathcal{H} T, \\ \tilde{\gamma} &= \gamma - L, \end{aligned} \quad (\text{A4})$$

where the conformal Hubble parameter is $\mathcal{H} = a'/a = aH$ and we denote the conformal time derivative as a prime. The vector metric perturbations transform as

$$\begin{aligned}\tilde{B}_\alpha &= B_\alpha + L'_\alpha, \\ \tilde{C}_\alpha &= C_\alpha - L_\alpha.\end{aligned}\quad (\text{A5})$$

Since tensor harmonics are independent of tensors that can be constructed from coordinate transformations, tensor-type perturbations remain unchanged under the gauge transformation.

Based on the gauge transformation properties, fully gauge-invariant quantities can be constructed as

$$\begin{aligned}\alpha_\chi &= \alpha - \chi'/a, \\ \varphi_\chi &= \varphi - H\chi, \\ v_\chi &= v + k\beta - k\chi/a,\end{aligned}\quad (\text{A6})$$

for scalar perturbations, where $\chi = a(\beta + \gamma')$ and $\tilde{\chi} = \chi - aT$. Our notation is chosen to facilitate the choice of gauge conditions [30], e.g., $\alpha_\chi = \alpha$, $\varphi_\chi = \varphi$, and $v_\chi = v$ in the conformal Newtonian gauge ($\beta = \gamma = 0$) or the zero-shear gauge ($\chi = 0$). For vector perturbations, two gauge-invariant quantities are

$$\begin{aligned}\Psi_\alpha &= B_\alpha + C'_\alpha, \\ \mathcal{V}_\alpha &= v_\alpha - B_\alpha,\end{aligned}\quad (\text{A7})$$

and we have used $V_\alpha = v_{\chi,\alpha} + \mathcal{V}_\alpha$ in the text. These gauge-invariant variables correspond to Φ_A , Φ_H , $v_s^{(0)}$, Ψ , and v_c in Bardeen's notation [24]. In addition to these gauge-invariant variables, one can construct other gauge-invariant variables, e.g., $\delta_v = \delta + 3(1+w)\mathcal{H}(v+k\beta)/k$, where $\delta_v = \delta$ in the comoving gauge, and indeed there are as many possibilities for gauge-invariant variables as for the choice of gauge condition.

Due to the spatial homogeneity of the background universe, all the perturbations should be invariant under pure spatial gauge transformations ($T = 0$, $\mathcal{L}^\alpha \neq 0$). Therefore, those perturbation variables ($\beta, \gamma, B_\alpha, C_\alpha$) that transform with L or L_α carry unphysical gauge freedoms and they can appear in physical quantities only through the combinations χ and Ψ_α that are invariant under spatial gauge transformations [31]. When the observed mean is subtracted from the observed number density field in Secs. II and III, these perturbation variables ($\beta, \gamma, B_\alpha, C_\alpha$) may leave unphysical gauge freedoms in the observed fluctuation field ruining its gauge-invariance. Fortunately, the damage is relatively innocuous, affecting only the monopole and the dipole at origin. In the paper, we explicitly resolve this issue by rearranging physical quantities in terms of spatially gauge-invariant combinations χ and Ψ_α , before any operation is taken.

Appendix B: Derivation of the Gauge-Invariant Equations

Here we derive the gauge-invariant equations used in the power spectrum analysis. The derivation closely follows our previous work [20], but we pay particular attention to

the gauge-invariance of perturbation variables of the observable quantities. Unphysical gauge terms are isolated and removed by expressing observable quantities in terms of gauge-invariant variables defined in Appendix A.

We parametrize the photon geodesic $x^a(v)$ in terms of the affine parameter v , and its wavevector is

$$k^a(v) = \frac{dx^a}{dv} = \left[\frac{\bar{\nu}}{a} (1 + \delta\nu), -\frac{\bar{\nu}}{a} (e^\alpha + \delta e^\alpha) \right], \quad (\text{B1})$$

where $\bar{\nu}$ and e^α represent the photon frequency and the photon propagation direction measured from the observer in the homogeneous universe. The null condition ($k^a k_a = 0$) for the wavevector constrains the zeroth order propagation direction $e^\alpha e_\alpha = 1$, and the geodesic equation ($k^b k_{;b}^a = 0$) yields $\bar{\nu} \propto 1/a$ and $e'^\alpha = e^\beta e_{|\beta}^\alpha$.

The dimensionless perturbations to the wavevector $k^a(v)$ are represented as $\delta\nu$ and δe^α for each component of Eq. (B1), and for the coordinate transformation in Eq. (A3) these perturbation components of the wavevector transform as

$$\begin{aligned}\tilde{\delta\nu} &= \delta\nu + \frac{d}{d\lambda} T + 2\mathcal{H}T, \\ \tilde{\delta e}^\alpha &= \delta e^\alpha + 2\mathcal{H}T e^\alpha - T e'^\alpha - \frac{d}{d\lambda} \mathcal{L}^\alpha - e_{;\beta}^\alpha \mathcal{L}^\beta,\end{aligned}\quad (\text{B2})$$

where $d/d\lambda = \partial_\tau - e^\alpha \partial_\alpha$ and it is related to the zeroth order photon path $d/dv = k^a \partial_a = (\bar{\nu}/a)(d/d\lambda)$. Based on the gauge transformation properties, we define two gauge-invariant variables for the wavevector as

$$\begin{aligned}\delta\nu_\chi &= \delta\nu + 2H\chi + \frac{d}{d\lambda} \left(\frac{\chi}{a} \right), \\ \delta e_\chi^\alpha &= \delta e^\alpha + 2H\chi e^\alpha - \left(\frac{\chi}{a} \right) e'^\alpha - \frac{d}{d\lambda} \mathcal{G}^\alpha - e_{;\beta}^\alpha \mathcal{G}^\beta,\end{aligned}\quad (\text{B3})$$

where $\mathcal{G}^\alpha = \gamma'^\alpha + C^\alpha$ is a pure gauge term, transforming as $\tilde{\mathcal{G}}^\alpha = \mathcal{G}^\alpha - \mathcal{L}^\alpha$.

The dimensionless perturbations $\delta\nu$ and δe^α to the wavevector are also subject to the null condition and satisfy the geodesic equation. In terms of the gauge-invariant variables, the null condition is

$$e_\alpha \delta e_\chi^\alpha = \delta\nu_\chi + \alpha_\chi - \varphi_\chi - \Psi_\alpha e^\alpha - C_{\alpha\beta} e^\alpha e^\beta, \quad (\text{B4})$$

and the temporal and spatial components of the geodesic equation are

$$\frac{d}{d\lambda} (\delta\nu_\chi + 2\alpha_\chi) = (\alpha_\chi - \varphi_\chi)' - (\Psi_{\alpha|\beta} + C'_{\alpha\beta}) e^\alpha e^\beta, \quad (\text{B5})$$

and

$$\begin{aligned}(\delta e_\chi^\alpha + 2\varphi_\chi e^\alpha + \Psi^\alpha + 2C_\beta^\alpha e^\beta)' \\ - e^\gamma (\delta e_\chi^\alpha + 2\varphi_\chi e^\alpha + \Psi^\alpha + 2C_\beta^\alpha e^\beta)_{|\gamma} \\ = \delta e_\chi^\beta e_{|\beta}^\alpha - \delta\nu_\chi e'^\alpha + (\alpha_\chi - \varphi_\chi)^{|\alpha} - \Psi_\beta^{|\alpha} e^\beta - C_{\beta\gamma}^{|\alpha} e^\beta e^\gamma,\end{aligned}\quad (\text{B6})$$

respectively. Fictitious gauge freedoms in $\delta\nu$ and δe^α are completely removed, and Eqs. (B4), (B5), and (B6) are manifestly gauge-invariant.

As our observable quantities are obtained by measuring photons from galaxies, we are mainly interested in perturbations along the photon geodesic given observed redshift z and observed angle $\hat{\mathbf{n}}$. Therefore, when we consider a coordinate transformation with the observable quantities fixed, the affine parameter λ is also affected by the coordinate transformation in Eq. (A3), i.e.,

$$\tilde{x}^a(\tilde{\lambda}) = x^a(\lambda) + \xi^a(\lambda), \quad (\text{B7})$$

and the deviation of the photon geodesic is

$$\widetilde{\delta x^a} = \delta x^a + \xi^a - \bar{k}^a \frac{a}{\bar{\nu}} \delta\lambda, \quad (\text{B8})$$

where $\delta\lambda = \tilde{\lambda} - \lambda$ and $\widetilde{d\lambda} = d\lambda(1 - 2\mathcal{H}T)$. The time lapse and the spatial shift are

$$\begin{aligned} \widetilde{\delta\tau_o} &= \delta\tau_o + T_o, \\ \widetilde{\delta x_o^\alpha} &= \delta x_o^\alpha + L_o^\alpha, \end{aligned} \quad (\text{B9})$$

at the origin $\lambda = \lambda_o$ and

$$\begin{aligned} \widetilde{\delta\tau_s} &= \delta\tau_s + T_s - \delta\lambda_s, \\ \widetilde{\delta x_s^\alpha} &= \delta x_s^\alpha + L_s^\alpha + e^\alpha \delta\lambda_s, \end{aligned} \quad (\text{B10})$$

at the source $\lambda = \lambda_s$, where the subscripts represent that the quantities are evaluated at the origin $x^a(\lambda_o)$ or the source position $x^a(\lambda_s)$.

A comoving observer with the four velocity $u^a = [(1 - \alpha)/a, v^\alpha/a]$ measures the redshift parameter z from galaxies and it is related to the photon wavevector as

$$\begin{aligned} 1 + z &= \frac{[k^a(\lambda_s)u_a(\lambda_s)]}{[k^a(\lambda_o)u_a(\lambda_o)]} \equiv \frac{1}{a_s}(1 + \delta z) \\ &= \frac{1}{a_s} \left\{ 1 + \mathcal{H}_o \delta\tau_o + \left[\delta\nu_\chi + \alpha_\chi + V - H\chi \right]_o^s \right\} \\ &= \frac{1}{a_s} \left\{ 1 - H\chi + (H_o\chi_o + \mathcal{H}_o\delta\tau_o) + \left[V - \alpha_\chi \right]_o^s \right. \\ &\quad \left. - \int_0^{r_s} dr \left[(\alpha_\chi - \varphi_\chi)' - (\Psi_{\alpha|\beta} + C'_{\alpha\beta}) e^\alpha e^\beta \right] \right\}, \end{aligned} \quad (\text{B11})$$

where r_s is the comoving line-of-sight distance to the source, $V = V_\alpha e^\alpha$ is the line-of-sight velocity, and $a_s = a[\tau(\lambda_s)]$. The redshift parameter z_h of the source, commonly defined as $1 + z_h = 1/a_s$, needs to be distinguished from the observed redshift z , and Eq. (B11) defines the lapse term δz in the observed redshift. Spurious spatial gauge freedom in δz is removed and its temporal gauge dependence is isolated $\widetilde{\delta z} = \delta z + \mathcal{H}T$. We define a gauge-invariant variable for the lapse in the observed redshift as $\delta z_\chi = \delta z + H\chi$.

The spatial displacement of the photon path can be obtained by integrating the spatial components of the geodesic equation in Eq. (B6) and using Eqs. (B9) and (B10). The radial displacement is

$$\delta r = e_\alpha x_s^\alpha - r_s \quad (\text{B12})$$

$$\begin{aligned} &= (\chi_o + \delta\tau_o) - \frac{\delta z_\chi}{\mathcal{H}} + \left[e_\alpha (\delta x_\chi^\alpha - \mathcal{G}^\alpha) \right]_o^s + \int_0^s d\lambda \delta\nu_\chi \\ &= (\chi_o + \delta\tau_o) - \frac{\delta z_\chi}{\mathcal{H}} - \left[e_\alpha \mathcal{G}^\alpha \right]_o^s \\ &\quad + \int_0^{r_s} dr (\alpha_\chi - \varphi_\chi - \Psi_\alpha e^\alpha - C_{\alpha\beta} e^\alpha e^\beta), \end{aligned}$$

where $(d/d\lambda) \delta x_\chi^\alpha = -\delta e_\chi^\alpha$. We have used the null condition for the wavevector in Eq. (B4) and defined the radial displacement δr with respect to the comoving line-of-sight distance r_s , slightly different from the definition used in [20]. Similarly, the angular displacements are

$$\begin{aligned} r_s \delta\theta &= \hat{\theta}_\alpha x_s^\alpha = \left[\hat{\theta}_\alpha (\delta x_\chi^\alpha - \mathcal{G}^\alpha) \right]_o^s \\ &= r_s \hat{\theta}_\alpha (\delta e_\chi^\alpha + \Psi^\alpha + 2C_\beta^\alpha e^\beta)_o - \left[\hat{\theta}_\alpha \mathcal{G}^\alpha \right]_o^s \\ &\quad - \int_0^{r_s} dr \left[\hat{\theta}_\alpha (\Psi^\alpha + 2C_\beta^\alpha e^\beta) \right. \\ &\quad \left. + \left(\frac{r_s - r}{r} \right) \frac{\partial}{\partial\theta} (\alpha_\chi - \varphi_\chi - \Psi_\alpha e^\alpha - C_{\alpha\beta} e^\alpha e^\beta) \right] \end{aligned} \quad (\text{B13})$$

and

$$\begin{aligned} r_s \delta\phi &= \hat{\phi}_\alpha x_s^\alpha = \left[\hat{\phi}_\alpha (\delta x_\chi^\alpha - \mathcal{G}^\alpha) \right]_o^s \\ &= r_s \hat{\phi}_\alpha (\delta e_\chi^\alpha + \Psi^\alpha + 2C_\beta^\alpha e^\beta)_o - \left[\hat{\phi}_\alpha \mathcal{G}^\alpha \right]_o^s \\ &\quad - \int_0^{r_s} dr \left[\hat{\phi}_\alpha (\Psi^\alpha + 2C_\beta^\alpha e^\beta) \right. \\ &\quad \left. + \left(\frac{r_s - r}{r \sin\theta} \right) \frac{\partial}{\partial\phi} (\alpha_\chi - \varphi_\chi - \Psi_\alpha e^\alpha - C_{\alpha\beta} e^\alpha e^\beta) \right], \end{aligned} \quad (\text{B14})$$

with the orthonormal direction vectors $\hat{\theta}$ and $\hat{\phi}$ perpendicular to the observed direction $\hat{\mathbf{n}}$. The gravitational lensing convergence is then defined as

$$\begin{aligned} \kappa &= -\frac{1}{2} \left[\left(\cot\theta + \frac{\partial}{\partial\theta} \right) \delta\theta + \frac{\partial}{\partial\phi} \delta\phi \right] \\ &= e_\alpha (\delta e_\chi^\alpha + \Psi^\alpha + 2C_\beta^\alpha e^\beta)_o - \int_0^{r_s} dr \frac{e_\alpha (\Psi^\alpha + 2C_\beta^\alpha e^\beta)}{r_s} \\ &\quad + \frac{1}{2r_s} \int_0^{r_s} dr \left[\hat{\theta}_\alpha \frac{\partial}{\partial\theta} + \frac{\hat{\phi}_\alpha}{\sin\theta} \frac{\partial}{\partial\phi} \right] (\Psi^\alpha + 2C_\beta^\alpha e^\beta) \\ &\quad + \int_0^{r_s} dr \left(\frac{r_s - r}{2rr_s} \right) \hat{\nabla}^2 (\alpha_\chi - \varphi_\chi - \Psi_\alpha e^\alpha - C_{\alpha\beta} e^\alpha e^\beta) \\ &\quad - \frac{1}{r_s} \left[e_\alpha \mathcal{G}^\alpha \right]_o^s + \frac{1}{2} \left[\hat{\theta}_\alpha \frac{\partial}{\partial\theta} + \frac{\hat{\phi}_\alpha}{\sin\theta} \frac{\partial}{\partial\phi} \right] \mathcal{G}^\alpha, \end{aligned} \quad (\text{B15})$$

where the Laplacian operator on a unit sphere is $\hat{\nabla}^2 = (\partial^2/\partial\theta^2) + \cot\theta(\partial/\partial\theta) + (1/\sin^2\theta)(\partial^2/\partial\phi^2)$. The presence of the gauge terms \mathcal{G}^α in Eqs. (B12)-(B15) explicitly indicates that the spatial displacements δr , $\delta\theta$, and $\delta\phi$ and the convergence κ are gauge-dependent, which can be understood as they represent the difference between the observed source position and the unobservable unlensed source

position and subsequently the function thereof. For notational convenience, we define two gauge-invariant quantities: $\delta\mathcal{R} = \delta r + [e_\alpha \mathcal{G}^\alpha]_o^s$ and $\mathcal{K} = \kappa + [e_\alpha \mathcal{G}^\alpha]_o^s / r_s - [\hat{\theta}_\alpha (\partial/\partial\theta) + (\hat{\phi}_\alpha / \sin\theta) (\partial/\partial\phi)] (\mathcal{G}^\alpha/2)$.

Finally, the volume occupied by the observed galaxies can be obtained by tracing backward the photon geodesic $x^\alpha(\lambda)$ given the observed redshift z and angle $\hat{\mathbf{n}}$, and the total number of galaxies in the observed volume is

$$\begin{aligned} N_{\text{tot}} &= \int \sqrt{-g} n_p \varepsilon_{abcd} u^d \frac{\partial x^a}{\partial z} \frac{\partial x^b}{\partial \theta} \frac{\partial x^c}{\partial \phi} dz d\theta d\phi \\ &= \int n_p \frac{r^2 \sin\theta}{(1+z)^3 H} dz d\theta d\phi \times \left[1 + 3\varphi \right. \\ &\quad + \Delta\gamma + v^\alpha e_\alpha + 3\delta z + 2\frac{\delta r}{r} + H\frac{\partial}{\partial z} \delta r \\ &\quad \left. + \left(\cot\theta + \frac{\partial}{\partial\theta} \right) \delta\theta + \frac{\partial}{\partial\phi} \delta\phi \right], \end{aligned} \quad (\text{B16})$$

where n_p is the physical number density of the source galaxies, the metric determinant is $\sqrt{-g} = a^4 (1 + \alpha + 3\varphi + \Delta\gamma)$, and ε_{abcd} is the Levi-Civita symbol. Equation (B16) means that N_{tot} is n_p times the physical volume described by the observed redshift z and angle $\hat{\mathbf{n}} = (\theta, \phi)$, and it defines the observed galaxy number density n_g as

$$N_{\text{tot}} = \int n_g \frac{r^2 \sin\theta}{(1+z)^3 H} dz d\theta d\phi, \quad (\text{B17})$$

providing the relation to the physical number density n_p .

With the contributions from the volume distortion between the observed and the physical, the observed galaxy number density has additional contributions from the physical galaxy number density, since more galaxies are observed along the overdense region due to the magnification given the threshold F_{thr} for the observed flux, and this source effect depends on the intrinsic luminosity function of the source galaxy population, $dn_p/dL \propto L^{-s}$: $n_p = n_p(L_{\text{thr}})(1 - 5p\delta\mathcal{D}_L)$, where the inferred luminosity threshold for the observed galaxies is $L_{\text{thr}} = 4\pi D_L^2(z) F_{\text{thr}}$, the luminosity function slope in magnitude is $p = 0.4(s - 1)$, and the luminosity distance in a homogeneous and isotropic universe is D_L .

Given the observed redshift z and angle $\hat{\mathbf{n}}$, the fluctuation $\delta\mathcal{D}_L$ in the luminosity distance \mathcal{D}_L , defined as $\mathcal{D}_L(z, \hat{\mathbf{n}}) = D_L(z)(1 + \delta\mathcal{D}_L)$, is [20, 32]

$$\begin{aligned} \delta\mathcal{D}_L &= \mathcal{H}_o \delta\tau_o + \left[\delta\nu + \alpha + (v_\alpha - \mathcal{B}_\alpha) e^\alpha \right]_s \\ &\quad + \frac{1}{r_s} \left(\delta\tau_s - \frac{\delta z}{\mathcal{H}_s} \right) - \int_0^{r_s} dr \frac{(r_s - r)r}{2r_s} \delta(\hat{R}_{ab} \hat{k}^a \hat{k}^b) \\ &= (\mathcal{H}_o \delta\tau_o + H_o \chi_o) + \left(\frac{\chi_o + \delta\tau_o}{r_s} \right) - \alpha_\chi + V - \frac{\delta z_\chi}{\mathcal{H} r_s} \end{aligned} \quad (\text{B18})$$

$$\begin{aligned} &- \int_0^{r_s} dr \frac{r}{r_s} \left[(\alpha_\chi - \varphi_\chi)' - (\Psi_{\alpha|\beta} + C'_{\alpha\beta}) e^\alpha e^\beta \right] \\ &+ \frac{1}{r_s} \int_0^{r_s} dr 2\alpha_\chi - \left[H_o \chi_o + H\chi - \frac{1}{r_s} \int_0^{r_s} dr 2H\chi \right. \\ &\quad \left. + \int_0^{r_s} dr \frac{(r_s - r)r}{2r_s} \delta(\hat{R}_{ab} \hat{k}^a \hat{k}^b) \right], \end{aligned}$$

and it is related to the magnification μ as $\mu = 1 - 2\delta\mathcal{D}_L$. The last term in Eq. (B18) is the source term for the expansion of the wavevector $\hat{\nu} = \hat{k}^a_{;a}$ in the conformally transformed metric $\hat{g}_{ab} = (\bar{\nu}/a)g_{ab}$ with the corresponding affine parameter λ ,

$$\begin{aligned} \delta(\hat{R}_{ab} \hat{k}^a \hat{k}^b) &= \Delta(\alpha_\chi - \varphi_\chi) - \alpha_{\chi, \alpha|\beta} e^\alpha e^\beta - 2\frac{d^2}{d\lambda^2} \varphi_\chi \\ &+ (\Psi'_{\alpha|\beta} e^\beta - \Delta\Psi_\alpha) e^\alpha + (C''_{\alpha\beta} - \Delta C_{\alpha\beta}) e^\alpha e^\beta, \end{aligned} \quad (\text{B19})$$

where \hat{R}_{ab} and Δ are the Ricci tensor and Laplacian operator of a three-space.

The last ingredient of our formalism is the linear bias approximation that relates the physical galaxy number density n_p to the underlying matter distribution ρ_m . Observationally, the time slicing is set by the observed redshift z and this choice is the only physical way in cosmological observations for defining the hypersurface of simultaneity without gauge ambiguity. The matter density at the observed redshift z of source galaxies is $\rho_m = \bar{\rho}_m(t)(1 + \delta_m) = \bar{\rho}_m(z)(1 + m_{\delta z})$ where $m_{\delta z} = \delta_m - 3\delta z$ and it is simply the matter fluctuation $m_{\delta z} = \delta_m$ in the uniform-redshift gauge ($\delta z = 0$). Therefore, the simplest linear bias ansatz we adopt is $n_p = \bar{n}_p(z)(1 + b m_{\delta z})$.

Finally the observed galaxy number density can be written in a manifestly gauge-invariant manner as

$$\begin{aligned} n_g &= \bar{n}_p(z) \left[1 + b m_{\delta z} + \alpha_\chi + 2\varphi_\chi + V \right. \\ &\quad - C_{\alpha\beta} e^\alpha e^\beta + 3\delta z_\chi + 2\frac{\delta\mathcal{R}}{r_s} \\ &\quad \left. - H\frac{\partial}{\partial z} \left(\frac{\delta z_\chi}{\mathcal{H}} \right) - 5p\delta\mathcal{D}_L - 2\mathcal{K} \right], \end{aligned} \quad (\text{B20})$$

and this completes the derivation of Eq. (1). In Eq. (B20) $\bar{n}_p(z)$ is the mean galaxy number density in a homogeneous and isotropic universe, in a close analogy to $\bar{\rho}_m$, though we cannot predict a priori its functional form. Lastly, it is worth emphasizing that Eq. (B20) is valid to the linear order only in metric perturbations as it involves no linearization in the matter density fluctuation δ_m , and hence it is valid in principle deep in the Newtonian limit, where the validity of the linear bias approximation is, however, highly in suspect.